PROCEEDINGS OF SCIENCE

Spatial filtering using a multibeam receiver

Jonathon Kocz[*†]
Swinburne University of Technology
E-mail: jkocz@swin.edu.au

Frank Briggs
The Australian National University

John Reynolds
Commonwealth Scientific and Industrial Research Organisation

Spatial filtering has traditionally been the province of antenna arrays, where both the Radio Frequency Interference (RFI) and celestial signals appear at all receivers. In the implementation described here, spatial filtering techniques are applied to data taken with the 20 cm multibeam receiver on the Parkes 64 m dish. Here, each of the feeds has independent celestial signal and system noise, but common RFI.

The signal processing requirements of the technique are outside the capacity of the standard spectrometer for the multibeam receiver at the observatory. As a result, a customised baseband recoding system was used to record the raw voltage data to disk, which were then processed offline in software.

The results demonstrate that spatial filtering methods provide powerful tools for interference mitigation with an array feed receiver.

RFI mitigation workshop
29-31 March 2010
Groningen, the Netherlands

[*]Speaker.
[†]Based on work done at The Australian National University.

PoS(RFI2010)032

1. Introduction

As computing power increases, so does the bandwidth processed by radio astronomy instruments. This means observations increasingly stray outside protected radio astronomy bands in the RF spectrum. Spatial filtering is one method that has previously been successful in removing interference from data taken with a telescope array [1]. In this paper, spatial filtering is applied to an array feed receiver on a single dish. This differs from the traditional application in that only the interference is common to the different feeds. Each input observes a different point on the sky. Section 2 gives a brief overview of spatial filtering theory and section 2.1 explains an extension to the algorithm for the case of pulsar observations with a stable interfering source. Section 3 details the experimental setup and results, and section 4 the conclusions.

2. Spatial filtering

As the theory of spatial filtering is covered in detail in several papers (see for example [1, 2, 3, 4, 5]), only a brief overview will be given here.

Spatial filters use the relative arrival times of a signal at multiple sensors to identify and separate signals from different directions. Assuming a multibeam receiver with p independent, dual polarisation beams and a single interferer, there is one beam on source, modelled as

$$S_1(f) = g_{A_1}A_1(f) + g_{I_1}I(f) + N_1(f) \tag{2.1}$$

where g_{A_1} and g_{I_1} are the gain applied to the astronomical and interfering signal from feed one, A_1 is the astronomical signal of interest in feed one, $I(f)$ the interference, and N_1 the noise.

The remaining beams are represented by

$$S_i(f) = g_{I_i}I(f) + N_i(f) \tag{2.2}$$

where $i = 2, p$. These signals are arranged into a covariance matrix $\mathbf{C}$, with elements $\langle S_j S_k^* \rangle$, where $j,k = 1, p$. The brackets $\langle ... \rangle$ denote integration over a finite time interval, and $(.)^*$ complex conjugation. The covariance matrix can be decomposed into the eigenvector, eigenvalue multiplication

$$\mathbf{C} = \mathbf{U}\Lambda\mathbf{U}^H \tag{2.3}$$

where $\mathbf{U}$ is the eigenvector matrix, Λ the eigenvalue matrix and $(.)^H$ denotes the Hermitian transpose. The eigenvectors and eigenvalues can be partitioned into noise (N) and interference (I) space. The dimensionality of these spaces depends on the number of interferers. $\mathbf{U}_I$ is of dimension $p \times r$, where r is the number of interferers. Similarly, Λ is of dimension $r \times r$. The celestial signal of interest is generally small compared to the noise in the short integrations on which the filtering is applied, and is therefore carried in the noise subspace.

The interference can be removed from $\mathbf{C}$ by projecting out the interference subspace. This is done by creating a projection using either $\mathbf{U}_I$ (where the interference projection is $\mathbf{P}_I = \mathbf{U}_I\mathbf{U}_I^H$) or $\mathbf{U}_N$ (where the noise projection is $\mathbf{P}_N = \mathbf{U}_N\mathbf{U}_N^H$), and applying it to the covariance matrix. In the case of the interference projection the corrected matrix $\tilde{\mathbf{C}} = \mathbf{C} - \mathbf{P}_I\mathbf{C}\mathbf{P}_I$. For the noise projection case $\tilde{\mathbf{C}} = \mathbf{P}_N\mathbf{C}\mathbf{P}_N$.

These projections can also alter the data of interest. In the array case in particular it is necessary to track the projections and apply a correction for the changes made to the visibilities [1, 3]. In the case of the array feed receiver we are not seeking to make an image from the combined beams; however, typically there is some cross contamination between the interference and noise space, which can result in an accidental over-correction when the projections are applied to the covariance matrix. Methods for accounting for this are discussed in [6, 7]. In section 2.1 we discuss an extension of the spatial filtering algorithm for an array feed receiver that does not require this correction. These changes are particularly suited to the case where high time resolution is desired, in the presence of a slowly varying interferer.

2.1 Average filter implementation

One of the practical limitations of spatial filtering is that the constructed projections generally require integration of the order of milliseconds in order to gain an appropriate signature of the interferer to develop a covariance matrix of appropriate rank [7]. However, in the case of a sufficiently stable RFI source, a high SNR projection created over longer timescales can be applied to the data at the Nyquist rate.

The average covariance matrix $\overline{\mathbf{C}}$ is constructed by averaging the covariance matrix for t seconds, where t is selected based on the stability of the interference environment. This matrix is decomposed into its eigenvector and eigenvalue components as normal, from which the average projections $\overline{\mathbf{P}}_N$ and $\overline{\mathbf{P}}_I$ are created, giving $\overline{\mathbf{C}} = \overline{\mathbf{P}}_N\overline{\mathbf{C}}\overline{\mathbf{P}}_N + \overline{\mathbf{P}}_I\overline{\mathbf{C}}\overline{\mathbf{P}}_I$. We now take these projections and apply them to the covariance matrix formed at arbitrarily short timescales, giving the corrected short-integration covariance matrix $\tilde{\mathbf{C}}_N = \overline{\mathbf{P}}_N\mathbf{C}\overline{\mathbf{P}}_N$ or $\tilde{\mathbf{C}}_I = \mathbf{C} - \overline{\mathbf{P}}_I\mathbf{C}\overline{\mathbf{P}}_I$. As the filter integration time is kept short enough that the interference can be considered stationary, the correction of the data amounts to a coherent subtraction. In this way there is no additional noise introduced to the system by the process.

Using the averaged projections has several advantages. The SNR of the interferer is increased, allowing the eigenvectors to be well determined. This in turn allows construction of a high SNR filter. The high SNR filter is better at identifying and isolating the RFI and leaving the noise containing the signal of interest untouched, as the reduced noise causes less distortion of the filter coefficients. In the particular case of pulsar observations, if the pulsar duty cycle is known, the average covariance matrix can be constructed with these time samples removed, also reducing the impact of the projection on the astronomical signal of interest. Finally, if the long term projections do not contain any (or only fractional) information about the pulsar, they can be applied to interference free areas of the spectrum without damaging the signal. This reduces the need for an RFI detection algorithm [7].

3. Parkes multibeam experiment

To practically test the effectiveness of the average projections, observations of the Vela pulsar were taken with the multibeam receiver on the Parkes 64 m dish. The Parkes multibeam is a 13 feed dual polarisation receiver. The raw voltages from each polarisation for an 8 MHz bandwidth, centred at 1440 MHz, were recorded at 2-bit resolution for offline playback. This was necessary as the standard multibeam processing chain was unable to form the required covariances in real

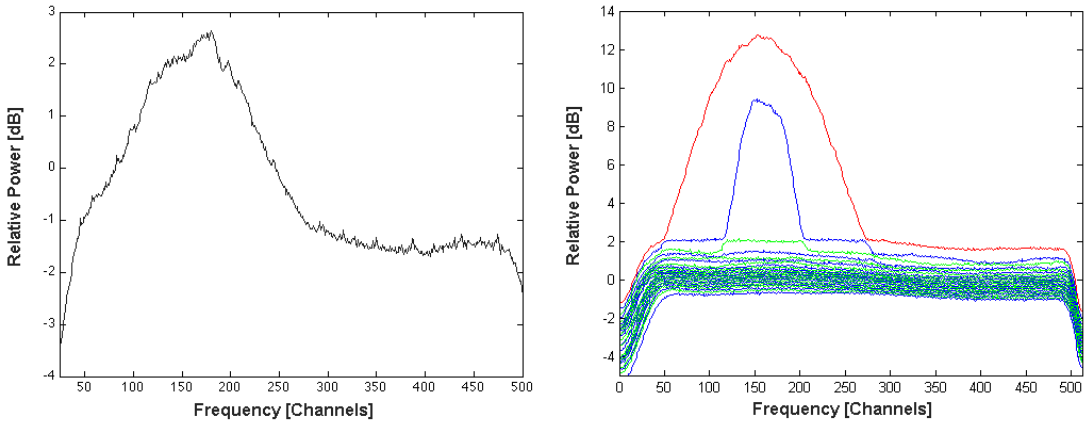

Figure 1: Left: The auto-correlation spectrum for the multibeam feed containing the Vela pulsar signal. The lower 4 MHz of the band are dominated by interference. Right: Eigenvalue spectra for the averaged covariance matrix. Eigenvalue 1 is in red, eigenvalues 2-26 are in alternating blue and green. The eigenvalues show that there are two main components to the interference. These correspond to two transmitters, one to the North, the other South at 1438.5 MHz.

time. The 8 MHz bandwidth was selected so that approximated half the band was contaminated by interference.

The data were processed using both traditional spatial filtering techniques, and also using the averaged projection matrices. Common to both methods, each of the 28 data lines were transformed into the frequency domain and auto- and cross-correlations were computed, with a spectral channel resolution of 15.625 kHz.

A 1 second average of the auto-correlation spectrum for the beam containing the pulsar, and the eigenvalue spectra for the averaged covariance matrix are shown in figure 1.

Following the theory outlined in section 2.1 the covariance matrix was formed and broken down into eigenvectors and eigenvalues on a 1 s timescale. For each covariance matrix, a projection of the interference was formed and applied.

Results were obtained for corrections of both the auto- and cross-correlation for the beam containing the pulsar, applying the projection in 1 ms steps, these are shown in figures 2 and 3. A slight dip in power following each pulse can be seen in the auto-correlation results. This is due to the presence of an automatic gain control (AGC) at the input to the digitizers in the processing chain. As the cross-correlation information is less effected by the AGC, and Vela is highly linearly polarized and easily detected in the cross-correlations, the results have been included as confirmation that the method does not corrupt the pulse data.

For the auto-correlation results, the SNR for an equivalent bandwidth in an interference free portion of the spectrum is 32.07, and for the cross-correlation case 28.91. The pre- and post-correction auto-correlation average SNR in the contaminated region was 5.07 and 26.91 and in the cross-correlation 3.04 and 20.86.

It is useful to note from figure 2 is that while the AGC does affect the data by varying the noise

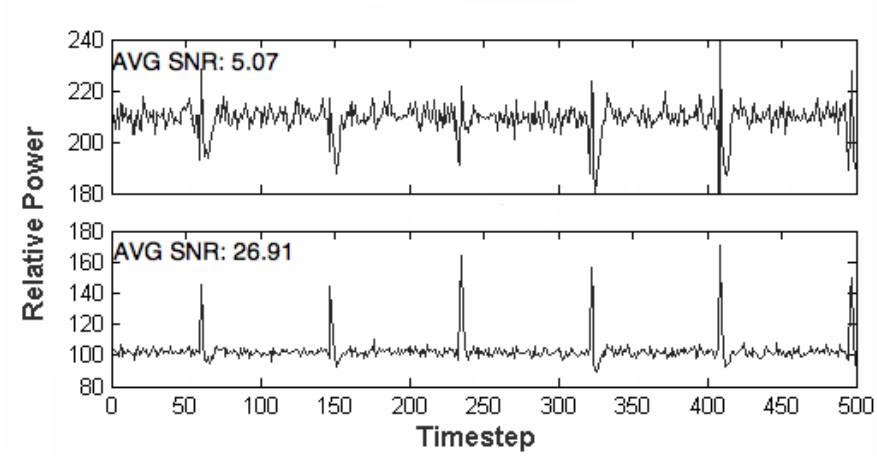

Figure 2: Timeseries formed from the auto-correlation spectrum showing the uncorrected (top) and corrected (bottom) power for part of the contaminated frequency range (spectral channels 100-250) at 1ms intervals.

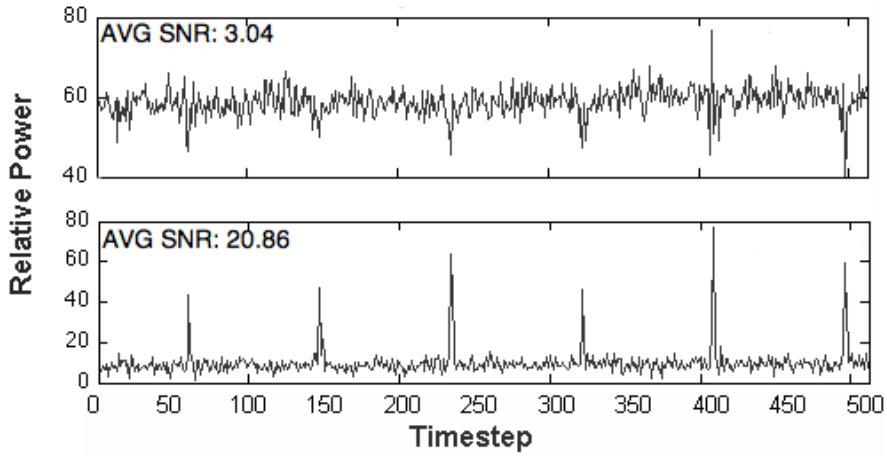

Figure 3: Timeseries formed from the cross-correlation spectrum showing the uncorrected (top) and corrected (bottom) power for part of the contaminated frequency range (spectral channels 100-250) at 1ms intervals.

and interference power level, the correction method is robust to this. This is because the changes in gains on the individual signal paths (here the AGC only affects the on pulse beam) are greatly reduced when calculating the projection [5, 7].

Calculations were also made using the original method, where the covariance matrix was computed and the projection created and applied for each 1 ms timestep. A correction was also used to account for any unwanted noise removal. These results gave a corrected average SNR of 16.54 for the cross-correlation case, indicating using the long term projections made a significant (26.35%) improvement in the correction. Also, while the results deteriorated when the projections were calculated and applied on timescales of less than 1 ms, the long term projections can be applied to

arbitrarily short timescales.

4. Conclusions

The results show that spatial filtering techniques can be successfully applied to an array feed receiver. Furthermore, the extension of the standard spatial filtering techniques to apply long term averages on short timescales was successful in increasing the SNR of pulsar pulses recovered from a highly contaminated area of spectrum.

References

[1] A. Leshem, A. van der Veen, A. Boonstra, *Multichannel Interference Mitigation techniques in Radio Astronomy*, *ApJS*, 131, 355, 2000.

[2] J. Raza, A. J. Boonstra, A. J. van der Veen,*Spatial filtering of RF interference in radio astronomy*, *IEEE Signal Processing letters*, vol 9, 2002.

[3] A. J. van der Veen, *Spatial filtering of RF interference in radio astronomy using a reference antenna*, *Proc. IEEE ICASSP*, pp. II. 189-193, 2004.

[4] A. J. Boonstra, *Radio frequency interference mitigation in radio astronomy*, *PhD thesis, Delft University of Technology*, 2005.

[5] J. Kocz, *Applied radio frequency interference removal in radio astronomy*, *PhD thesis, Australian National University*, 2009.

[6] D. Mitchell, *Interference mitigation in radio astronomy*, *PhD thesis, University of Sydney*, 2004.

[7] J. Kocz, F. Briggs, J. Reynolds, *Radio frequency interference removal through the application of spatial filtering techniques on the Parkes multibeam receiver*, *AJ, submitted*, 2010.